Hybrid Energy Storage System with Power Surge Capabilities Utilizing Six-Port Converter for Cell Management

Ilya Zeltser
Power Electronics Department
Rafael Advanced Defence Systems LTD.
P. O. Box 2250,
Haifa 31021, Israel
ilyaz@rafael.co.il

Michael Evzelman
Department of Electrical and Computer Engineering
Ben-Gurion University of the Negev
P. O. Box 653,
Beer Sheva 84105, Israel
evzelman@bgu.ac.il

Daniel Beniaminson
Department of Electrical and Computer Engineering
Ben-Gurion University of the Negev
P. O. Box 653,
Beer Sheva 84105, Israel
benidani@bgu.ac.il

Mor M. Peretz
Department of Electrical and Computer Engineering
Ben-Gurion University of the Negev
P. O. Box 653,
Beer Sheva 84105, Israel
morp@bgu.ac.il

***Abstract*—A hybrid energy storage architecture that consists of energy storage string of cells, typically lithium batteries, and power surge capable string of cells, typically supercapacitors is presented. The major challenge – cells management in a multi string multi cell system is tackled in this work by introducing a novel six-port converter, which on one hand enables to balance individual cells across each of the strings, while on the other hand provides a low power means of shuttling the charge between the strings as necessary. The unique converter topology uses capacitive coupling between the cells on the same string, and near unity conversion ratio isolated transformer coupling between the energy and power strings, providing single conversion high efficiency balancing operation and cutting significantly on the number of required components. A simulation and experimental validation of the converter operation and hybrid energy architecture functionality is carried out on a laboratory prototype, and a good agreement is found between the theoretical analysis and experimental results.**

Keywords—Energy storage, balancing, battery management.

I. INTRODUCTION

There is a fundamental limitation of batteries-based energy storage imposed by currently available technology, and it is a strict tradeoff between the peak current of the battery, and its storage capacity. For the same cell size, the higher the peak current the battery is rated for, the lower the amount of energy it stores [1-3]. There are several approaches to address the high-power demand in energy storage systems. One, is to size the batteries according to the peak power demand. This method results in a significantly oversized installation, which is underutilized in terms of energy storage, and financially prohibitive in many applications. Another approach is to maintain a fossil fuel-based backup, capable to take over the load in several seconds. This approach is prohibitive both financially and in terms of noise and pollution. An alternative approach, which is based on two types of energy cells combined into a single energy storage unit is explored in this work.

Energy storage unit hybridization on the string level could include fuel cells and super capacitors like in [4], or as explored in this study, a unit where the battery is complimented with a string of supercapacitors (Fig. 1), [5-7]. This hybrid energy storage unit is capable to provide both high energy capacity, utilizing a string of lithium-ion batteries, along with a high surge power capabilities utilizing a string of super capacitors. Super capacitors may be charged/discharged tens of thousands of times during their life span. It provides an excellent dynamic energy storage, prevent high current stresses on the batteries, and quick charge/discharge cycling, which has a potential to prevent accelerated battery degradation [8-9].

The dual string approach was previously investigated. Sizing and effectiveness quantification of the two cell strings was summarized [10-11]. However, there are additional challenges associated with hybridization of two strings. One of the major challenges is housekeeping of two large strings of serially connected DC cells and effective and efficient energy shuttling between them. Some previous works on the subject of hybrid storage units housekeeping on a string-by-string basis, attaching multiple converters to each cell for balancing and supervision were carried out in [12-15]. This challenge is further tackled in this work, by introducing a novel bidirectional six-port converter, which on one hand enables to balance individual cells across each of the strings, while on the other hand provides a low power means of shuttling the charge between the strings as necessary.

To maximize the current sourcing performance, while the batteries are partially discharged, a unique operating mode is introduced, which enables to retain maximum voltage across the power (capacitors') string at all times. The converter features lower component count and has better efficiency due to a reduced number of energy conversions that are required to reach each of the cells along the two strings.

The rest of the paper is organized as follows, section II introduces the topology, including the string equalizers, outlines the operation principle of basic balancing and the new mode, and presents topology analysis. Section III summarizes the simulation results, section IV details the experimental validation, and section V concludes the paper.

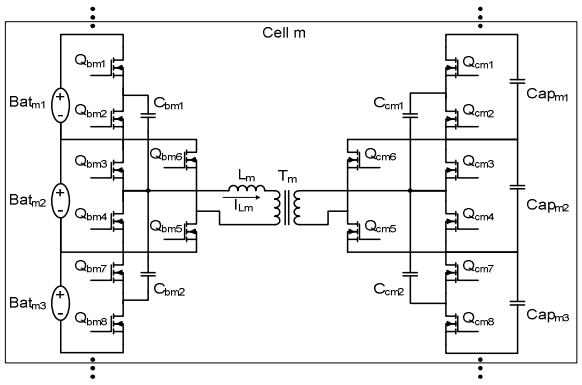

Fig. 1. Ballancing cell.

II. Operation and Analysis of the Equalizer

The system in Fig. 1 comprises the energy string $Bat_1 \ldots Bat_N$ and the power string $Cap_1 \ldots Cap_N$ that are divided into m equalization cells $Cell_1 \ldots Cell_m$. Each cell equalizes 3 batteries and 3 capacitors, such that $N = 3m$. The cell consists of four switching capacitors Cb_{m1}, Cb_{m2}, Cc_{m1} and Cc_{m2}; 16 transistors $Q_{bm1..8}$ and $Q_{cm1..8}$ on the batteries and on the capacitors sides, a series inductor L_m and a link transformer T_m. L_m can be implemented as a leakage inductance of the transformer T_m. The arrangement of the elements is shown in of Fig. 1. Normally, the voltages in both strings are equalized by transferring the charge from the stronger to a weaker battery or capacitor. In the proposed circuitry it is done by two independent channels.

One is responsible for balancing the voltages in the same string, and the second is used to transfer the energy between the strings. As a result, both strings are simultaneously balanced. The excessive charge along the strings is transferred by a pair of the switching capacitors ($C_{bm1,2}$ on the batteries side and $C_{cm1,2}$ on the capacitors side) and between them - through the inductor L_m and the transformer T_m.

Both charge exchanging channels are independent and controlled by the same simple switching sequence. The switching period, $1/f_s$, is divided into two half-cycles having an 'on' and an 'off' time each (Fig. 2, where k = 1,2…n). The odd-numbered transistors conduct during the 'on' time of the first half-cycle (t_1-t_2) whereas the even-numbered transistors are engaged during the 'on' time of the second half-cycle (t_3-t_4).

At the 'off' times (t_2-t_3, t_4-t_5) all the transistors are switched off. The switching capacitor C_{bm1} is switched between the upper battery Bat_{m1} and the middle battery Bat_{m2}, and C_{bm2} is switched between Bat_{m2} and the lower battery Bat_{m3}, transferring the charge between them. Similarly, on the capacitors string side, C_{cm1} is switched between Cap_{m1} and Cap_{m2} whereas C_{cm2} transfers the charge between Cap_{m2} and Cap_{m3}. This is demonstrated in Fig. 3, that shows the connections of the switching capacitors to the corresponding storage units, during the 'on' times (t_1-t_2, t_3-t_4). It should be noticed that no energy is transferred along the strings if the batteries or capacitors are balanced, reducing the losses associated with the reactive currents. The time it takes to equalize the voltages between the adjacent storage capacitors can be evaluated assuming, that the equalization is accomplished, when the voltage difference between the two capacitors converges to less than, say, 1% of their initial value. Then, the conversion time in the capacitors' string can be estimated as:

$$t_{conv_{str}} \approx \frac{2.5 C_{st}}{f_s C_{sw}} \qquad (1)$$

where C_{sw} is the capacitance of the switching capacitor (C_{cm1} or C_{cm2}).

(It should be noticed that the conversion time on the batteries' side depends on the charge-to-voltage curve of the batteries at hand and therefore is not estimated here.)

The energy transfer to the capacitors' string resembles the operation of the capacitor charger with triangular shaped inductor current [5, 6]. It is done between the middle battery Bat_{m2} and the middle capacitor Cap_{m2} through the inductor L_m and the transformer T_m, as shown in Figs. 4 and 5. Assuming

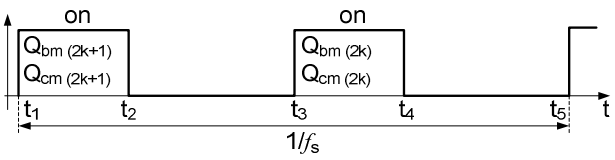

Fig. 2. Switching sequence of the balancing cell

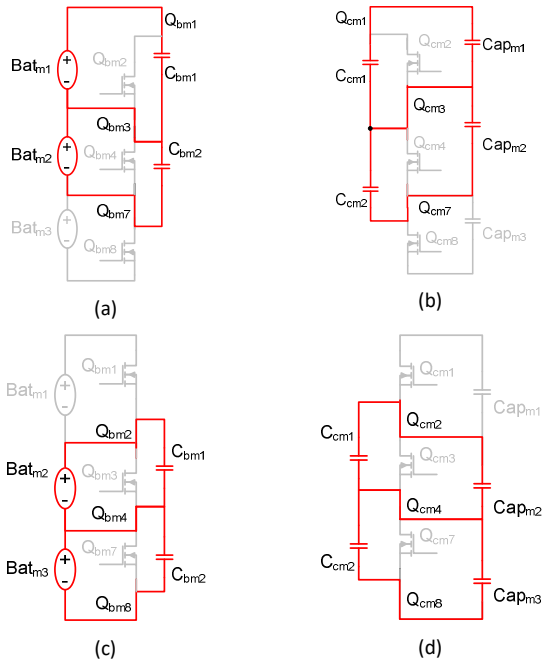

Fig. 3. Balancing along the strings. (a) t_1-t_2, battery string; (b) t_1-t_2, capacitors' string; (c) t_3-t_4, battery string; (d) t_3-t_4, capacitors' string.

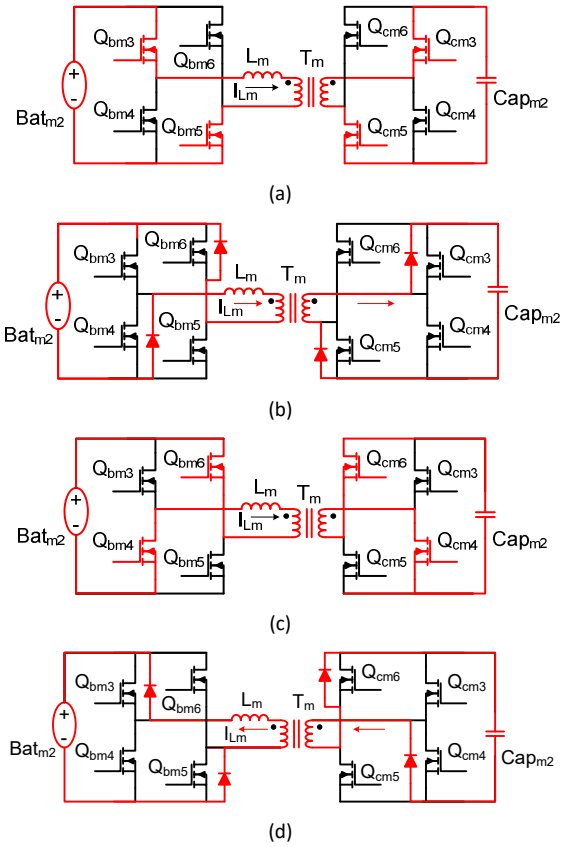

Fig. 4. Operating modes of the proposed circuit. (a) t_1-t_2, (b) t_2-t_3, (c) t_4-t_5, (d) t_5-t_6.

the transformer ratio of unity, the voltage, seen by the inductor L_m during the time interval t_1-t_2 (Fig. 2, 4a), is (V_{BATm2}-V_{CAPm2}). No energy is transferred if the voltages of the battery Bat_{m2} and of the capacitor Cap_{m2} are equal.

At t_2 the transistors are turned off and the inductor's current flows through the anti-parallel diodes of Q_{bm4}, Q_{bm6}, Q_{cm3}, Q_{cm5} (or via the transistors in case of synchronous operation, Fig. 4b) and the voltage, applied to the inductor, is $-(V_{Bat\ m2}+V_{Cap\ m2})$. The polarity of the voltage applied to the inductor during t_2-t_3 is inverted, bringing the inductor's current back to zero at t_3, before the beginning of the subsequent half-cycle.

The operation of the circuit during the second half-cycle (t_4-t_6) is similar (Fig. 4c-4d), except that the voltage applied to the transformer is negative. This way the magnetization current of the transformer is reset.

It is assumed, that the voltages of the storage elements over the switching cycle remain unchanged. Next, the time intervals (t_2-t_1)=(t_5-t_4) and (t_3-t_2)=(t_6-t_5) are denoted as t_{on} and t_{off}, in accordance. Then, the inductor's current, I_{Lm}, averaged over the switching period is:

$$I_{Lm\,av}(t) = \frac{V_{BATm2}-V_{CAPm2}(t)}{L_m} t_{on}\left(t_{on} + t_{off}\right) f_s \quad (2)$$

Considering volt-second balance of the inductor one gets:

$$\frac{t_{off}}{t_{on}} = \frac{V_{BATm2}-V_{CAPm2}(t)}{V_{BATm2}+V_{CAPm2}(t)} \quad (3)$$

Substituting (3) back into (2) yields:

$$I_{Lm\,av}(t) = V_{BATm2}\frac{2t_{on}^2 f_s}{L_m} \cdot \frac{V_{BATm2}-V_{CAPm2}(t)}{V_{BATm2}+V_{CAPm2}(t)} \quad (4)$$

For a unity gain transformer, this current is equal to the current through the capacitor Cap_{m2} and hence, the capacitor's voltage over the charging period can be found considering its characteristic equation, that is:

$$\frac{dV_{CAPm2}}{dt} = \frac{I_{Lm\,av}(t)}{C_{st}} \quad (5)$$

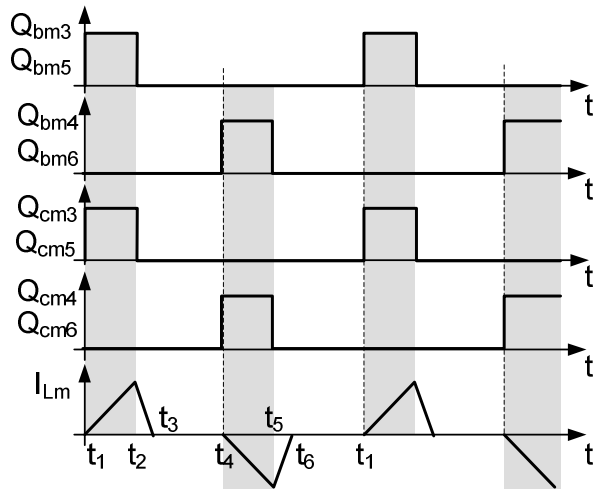

Fig. 5. Key waveforms of the proposed circuitry

Substituting in (4) and rearranging yield a separable differential equation of the following form:

$$\frac{1+G(t)}{1-G(t)} dG(t) = \frac{t}{\tau_p} \quad (6)$$

where: G(t) is the capacitor-to-battery voltage ratio over the equalization period, so that:

$$G(t) = \frac{V_{CAPm2}(t)}{V_{BATm2}} \quad (7)$$

and τ_p is defined as follows:

$$\tau_p = \frac{C_{st} \cdot L_m}{2 \cdot t_{on}^2 \cdot f_s} \quad (8)$$

G(t) is obtained by integrating both sides of (6), that is:

$$2 \cdot \ln\left(\frac{1-G(t)}{1-R}\right) + G(t) - \mathrm{R} = -\frac{t}{\tau_p} \quad (9)$$

where R is defined as capacitor-to-battery voltage ratio at the beginning of the equalization period, i. e. $R = G(0)$.

Assuming, that the equalization is accomplished when the capacitor V_{CAPm2} is charged to the 99% of its target value, that is $0.99V_{BATm2}$, the battery-to-capacitor conversion time is calculated as follows:

$$t_{conv_{link}} = \tau_p[8.22 + R + 2 \cdot \ln(1-R)] \quad (10)$$

The maximum conversion time will be observed when the capacitor Cap_{m2} is fully discharged, so the upper limit for the conversion period is obtained from (10) by letting R=0, as follows:

$$t_{link_{max}} = 8.22 \cdot \tau_p \quad (11)$$

In practical applications, the nominal voltages of the batteries and of the capacitors, used in the storage unit, are not necessarily identical. For example, the operating voltage of LiIon batteries can be as high as 4.2V whereas the nominal voltage of the super capacitors is usually confined to 2.7V. Assuming that the LiIon batteries and the super capacitors are chosen for the energy and for the power storage strings, their voltages cannot be equalized. This can be resolved by adjusting the transformer ratio of the Tm. That is, if, in the above example, the primary-to-secondary ratio of the transformer is set to about 1.6 (~4.2V/2.7V), the storage elements in both strings will operate at their nominal voltages.

In the arrangement above the voltages across the storage capacitors follow the voltage of the batteries and therefore decrease when the batteries discharge. This impairs the peak current performance of the storage unit at low state-of-charge of the batteries.

Assuming a fast load change, such that all the current is consumed from the storage capacitors, the maximum current that the storage unit can provide during this transient is calculated as follows:

$$I_{av} = \frac{C_{string}(V_{string}-V_{min})}{\Delta t} \quad (12)$$

where – I_{av} is the maximum output current averaged over the transient time, C_{string} is the overall capacitance of the capacitors string, V_{string} is the voltage across the string before the load change, V_{min} is the minimum allowable load voltage, Δt is the transient time of the load. For V_{min} of, say, 70% of the nominal voltage, and assuming that V_{string} was kept at 80% of its nominal value prior to a load change, the maximum current that can be drawn from the storage unit will be 3 times lower compared to the case of the maximum (nominal) voltage across the storage capacitors. To preserve the current sourcing performance of the storage unit over the discharge cycle of the batteries, the switching sequence of the arrangement of Fig. 1 can be modified to keep the storage capacitors at their nominal voltage, regardless of the state-of-charge of the batteries. It is done by introducing a phase shift to the gate signals of the transistors Q_{cm5}, Q_{cm6} as demonstrated in Fig. 6. Fig. 7 shows the operating modes of the proposed circuit while applying the modified switching sequence. During the time intervals (t_1-t_2) and (t_4-t_5) the secondary winding of the transformer is shorted, so the voltage applied to the inductor is $\pm V_{bat\,m2}$, and the current in the inductor raises (Fig. 7a and 7c). During the time intervals (t_2-t_3) and (t_5-t_6) the voltage across the inductor is given by the voltage difference of the battery Bat_{m2} and of the storage capacitor Cap_{m2}, ($V_{BATm2} - V_{CAPm2}$). Consequently, for the inductor's current to decrease (Fig. 7b and 7d,) the $V_{Cap\,m2}$ must be higher than the voltage on the battery. In other words, the average voltage of the inductor L_m (see (13)), can only be zero if $V_{CAPm2} > V_{BATm2}$.

$$V_{L\,av} = V_{BATm2}(t_2 - t_1) + (V_{BATm2} - V_{CAPm2})(t_3 - t_2) \quad (13)$$

When the capacitors' string is not loaded, its voltage will only increase and therefore, the application of this switching sequence calls for an active control of the voltage across the capacitors' string. One of the simplest control schemes can be the hysteretic control, that is, once the voltage across the storage capacitors have reached their target value, the transistors Q_{bm5}-Q_{bm6} are switched off and remain so until the voltage across the capacitors' string drops back below the predefined threshold.

It is worth emphasizing that boosting the voltage of the capacitors' string does not affect the equalization process across the strings.

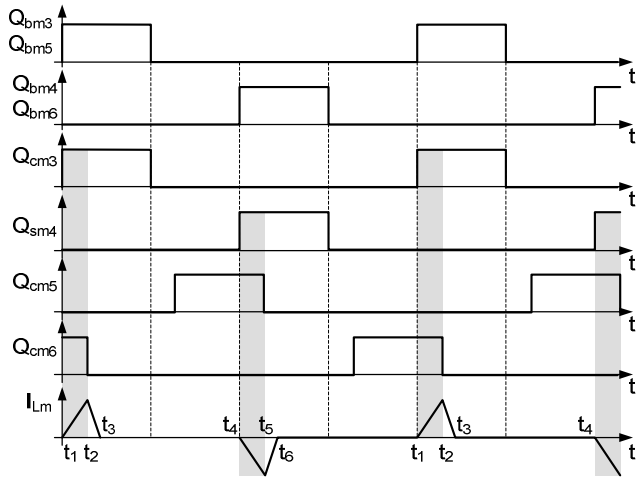

Fig. 6. Key waveforms of the proposed circuitry applying a switching sequence with a phase shift

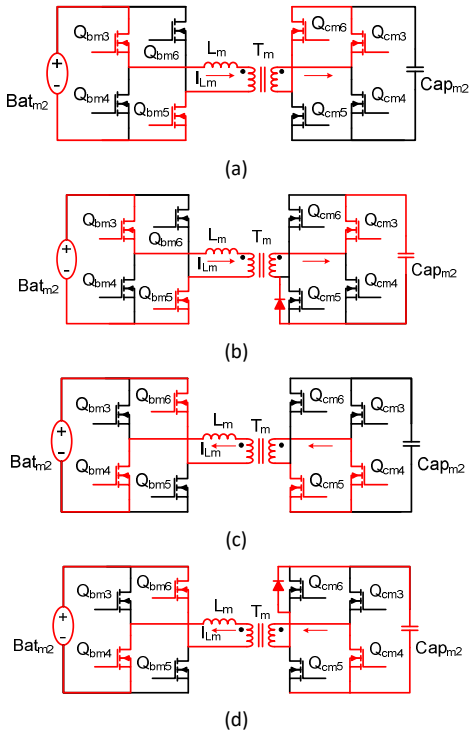

Fig. 7. Operating mode of the proposed circuit applying phase shift sequence. (a) t_1-t_2, (b) t_2-t_3, (c) t_4-t_5, (d) t_5-t_6.

III. Simulation Results

The equalization circuit presented in this work has been verified by simulation model (Fig. 8.). The notations of the elements in Fig. 8 correspond to those in Fig. 1. To shorten the simulation runtime the batteries and the storage capacitors are modeled in Fig. 6 by relatively small capacitors of 10 µF. The transformer ratio is set to n1:n2 = 1.6. The maximum voltages of the batteries and the storage capacitors are designed to be 4.2V and 2.7V respectively. Figure 9 shows the convergence of the balancing cells from different initial voltage values. The envelope of the inductor current L_m decreases and finally drops to zero as the voltages of the batteries and the storage capacitors approach their final values, attesting that no reactive energy is exchanged among the strings when their voltages are equalized. Fig. 10 demonstrates the behavior of the balancing circuit when the 'batteries' are partially discharged. Here, the voltage of the middle storage capacitor is sensed (Fig. 8), and phase shifted sequence is engaged to boost the capacitor's voltage up to the predefined value of 2.65V. Once the middle capacitor (CAPm2) reaches the 2.65V, the output of the comparator A1 goes low and the transistors Q_{bm5} and Q_{bm6} are switched off (by MUX1 and MUX2), so that no energy is passed between the strings.

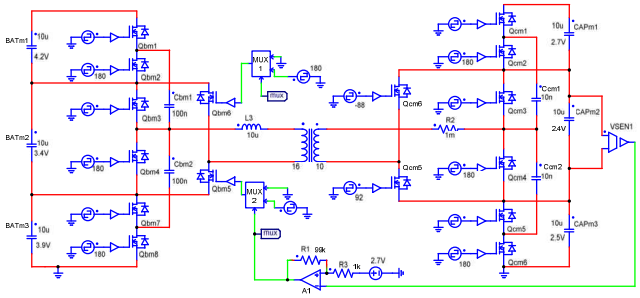

Fig. 8. Simulation circuit.

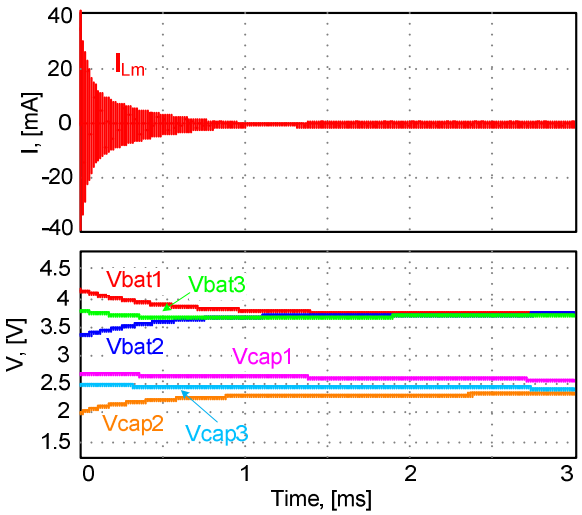

Fig. 9. Conversion of the storage elements.

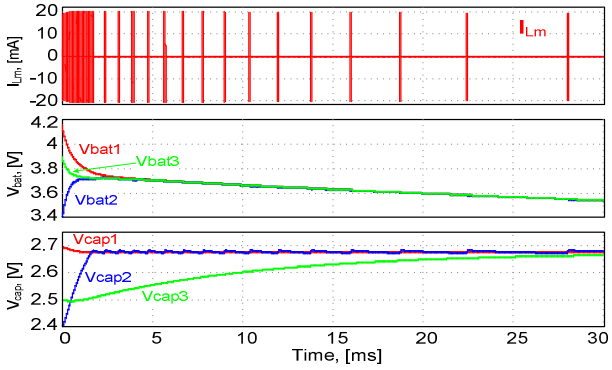

Fig. 10. Keeping storage capacitors at nominal voltage.

IV. EXPERIMENTAL RESULTS

An experimental prototype of the hybrid energy storage system presented in this work is shown in Fig. 11. The left side of the prototype includes energy optimized string of cells, batteries in this case, and the right side of the prototype includes electrolytic capacitors, which constitute a power capable string of cells. The switches BSC015NE2LS5IATMA1 by Infineon are used in both strings. The switching frequency is set to 225kHz. The central part of the PCB includes the connection link between the strings, built around a 1:1 transformer according to the schematic of Fig. 1. The transformer's leakage inductance of 400nH is utilized as a series inductor.

To validate the operation of the hybrid energy storage four experiments are carried out. The first experiment demonstrates independent balancing operation of each of the strings. To shorten the runtime of the experiment, the energy string batteries are substituted with electrolytic capacitor of 12.2mF. The experiment begins with manual charging of the bottom #1, middle #2, and top #3 cells to initial voltages V_0 of 3.6V, 4.15V and 2.9V respectively, and the balancing system is enabled to run. The results are shown in Fig. 12. Each trace represents the voltage of one of the cells. The traces converge to a common average value after a short period. There is a minor difference less than 30mV.

A second experiment demonstrates the advantage potential of hybrid energy storage design, where high power capable string is connected in parallel to an energy storage string and to the load located on the same bus. In this trial

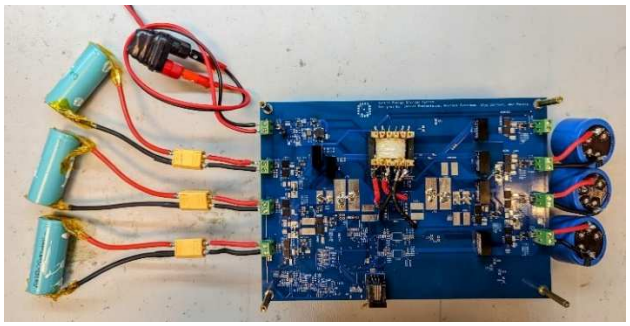

Fig. 11. Experimental prototype photograph.

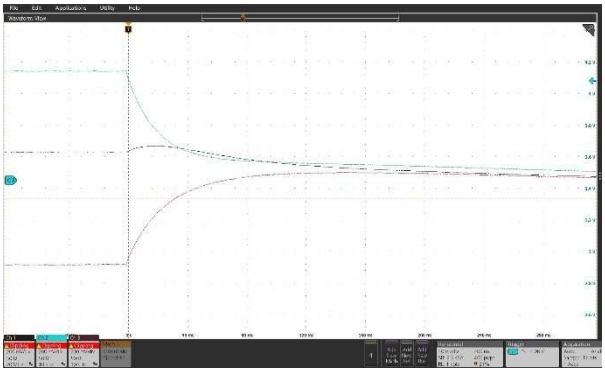

Fig. 12. Balancing operation. Horizontal scale: 40ms/DIV; Vertical scale: 200mV/DIV. Top (blue) trace – cell #2, V_0 = 4.15V; middle (black) trace – cell #1, V_0 = 3.6V; bottom (red) trace – cell #3, V_0 = 2.9V.

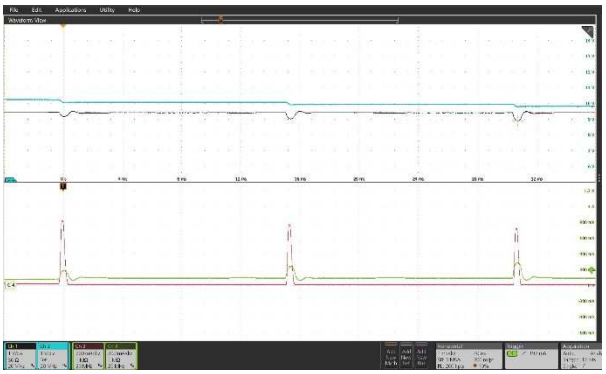

Fig. 13. Load response of the hybrid energy storage. Horizontal scale: 4ms/DIV; Top (blue) trace – capacitor voltage; second from the top (black) trace – bus and load voltage; Vertical scale: 1V/DIV. Bottom (red) trace – capacitor current; Second from bottom (green) trace – batteries current; Vertical scale: 200mA/DIV.

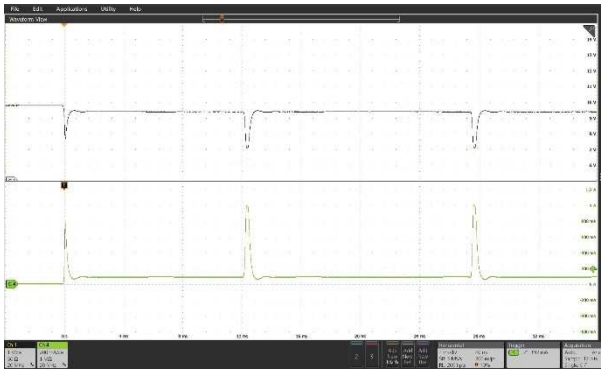

Fig. 14. Load response of a conventional energy storage. Horizontal scale: 4ms/DIV; Top (black) trace – bus and load voltage; Vertical scale: 1V/DIV. Bottom (green) trace – batteries current; Vertical scale: 200mA/DIV.

some older, high impedance, second-life rated LFP battery cells were used to implement a high energy low power capable string, and a string of 5.6mF capacitors was used as a power capable string. For the matter of demonstration, the connection between the batteries and the capacitors to the load was implemented using diodes, the final design could use a different bus connection approach. Experimental hybrid energy storage was exposed to a 0.1A continuous current load, which was drawn from the energy storage string, and some peak current demands of 1A were introduced for short durations of 1ms, with a period of 15ms. The results of bus voltage and currents drawn from each of the strings are summarized in Fig. 13. The top trace is the capacitors string voltage, second top trace is the bus voltage, were during the current peak spikes a small voltage dip of 200mV is present. The bottom green trace is the battery current, and the red trace is the capacitors current. The continuous load current is as expected supplied by the batteries. During the high current demand events, as the voltage across the bus dips below the conduction voltage of the diode, capacitors are stepping in and provide most of the current required by peak current demand events. Batteries current increases during the peak power demand, however the increase is only twice comparing to the continuous system operation, maintaining the discharge rates well within the battery limits, and avoiding battery life shortening events. The capability of the batteries to provide current without using the capacitors bus are shown in Fig. 14. Bus voltage experiences large voltage drops due to a limited batteries capability, and high internal impedance.

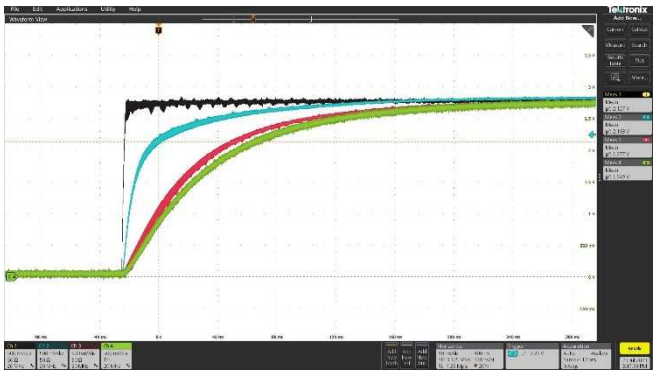

Fig. 15. Energy transfer between strings in a simple balancing mode. Horizontal scale: 40ms/DIV; Vertical scale: 500mV/DIV. Top (black) trace - batteries voltage; Second top (blue) trace – middle capacitor; Third top (red) trace – top capacitor; Bottom (green) trace – bottom capacitor.

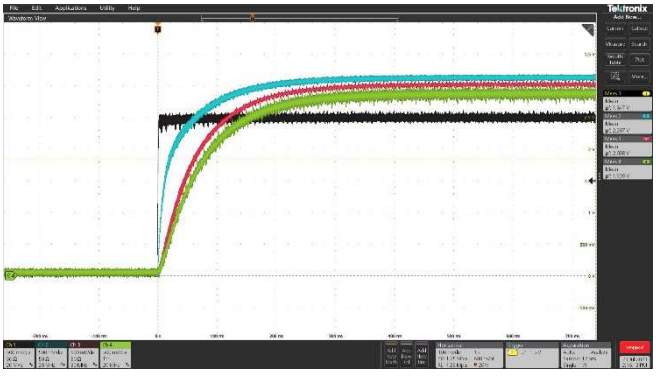

Fig. 16. Energy transfer between strings in a boost mode. Horizontal scale: 100ms/DIV; Vertical scale: 500mV/DIV. Top (blue) trace – middle capacitor; Second top (red) trace – top capacitor; Third (green) trace – bottom capacitor; Bottom (black) trace – batteries voltage.

Third experiment demonstrates the operation of energy connection link between the two strings in a simple balancing mode, according to the switching sequence of Fig. 5. The batteries at the energy string were charged to 2.8V, while the capacitors string was completely discharged. The balancing circuits and strings connection link were enabled before instantaneously connecting the energy string to the board. The resulting response of the system is shown in Fig. 15, where the top (black) trace is the central battery voltage (the batteries were balanced at this point), the second from the top trace (blue) is the middle capacitor, the third from the top trace (red) is the top capacitor, and the bottom trace (green) is the bottom capacitor. Two parallel processes are taking place in this case. One, is the middle capacitor begins to receive energy from the batteries through the string connection link. Since the string linking converter runs here in a simple balancing mode according to the switching sequence of Fig. 5, middle capacitor begins to charge quickly to the same voltage as the batteries. The other process is the balancing between the capacitors. Top and bottom capacitors charge up to the battery's voltage as the middle capacitor, in a slower than middle capacitor pace, due to indirect charge transfer.

The fourth experiment demonstrates the operation of energy connection link between the two strings in a boost mode, according to the switching sequence of Fig. 6. The batteries at the energy string were charged to their very minimum voltage of 2.5V, to emulate a nearly depleted energy storage. The capacitors string was completely discharged. At this point a conventional energy storage system would be able to sustain some low-level continuous current for a short period of time, however even the smallest peak power demand on the bus, will result in a battery shutdown by the protection circuitry to avoid over-discharge, and associated permanent battery damage. To prevent this, in the hybrid energy storage system, demonstrated in this study, the capacitors are always kept charged at their maximum voltage by operating the string connection link in a boost mode (Fig. 6). This experiment demonstrates the charge up of the capacitors string to their maximum voltage 3.0V each, from the batteries that are at near depletion level of 2.5V. The response of the system is shown in Fig. 16, where the top trace (blue) is the middle capacitor, second from the top trace (red) is the top capacitor, third from the top trace (green) is the bottom capacitor, and the bottom trace is the voltage of the central battery (the batteries were balanced at this point). The energy from the

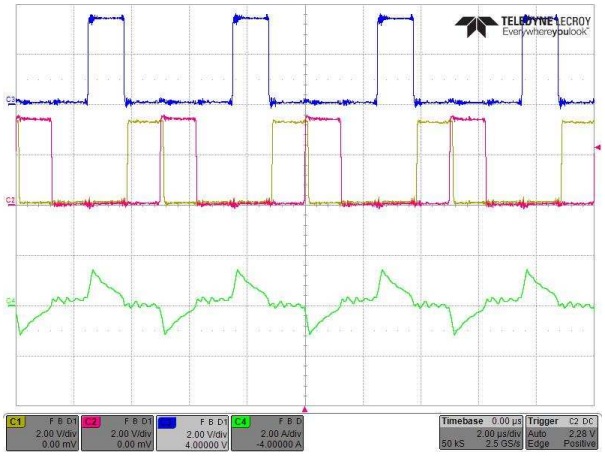

Fig. 17. Boost operation of strings linking converter. Gate signals of: Top (blue) trace – Q_{cm3}; Middle (yellow) trace – Q_{cm5}; Middle (red) trace – Q_{cm4}; Bottom (green) trace – transformer current 2A/DIV. Horizontal scale: 2µs/DIV.

batteries is passed to the middle capacitor, which is the quickest to charge, and then redistributed between the rest of the capacitors, which are charged at a slower rate.

The operation of the linking converter in a boosting mode is shown in Fig. 17. The top three traces are the gating signals. The top trace (blue) is Q_{cm3} (Q_{cm6} is complementary to it and is omitted), the middle traces are (yellow) Q_{cm5} and (red) Q_{cm4} that overlap due to a phase shift. The bottom trace (green) is the transformer current, which is similar to the current shown in the timing diagram of Fig. 6.

V. Conclusions

A hybrid energy storage architecture that consists of energy storage and power surge capable strings of cells is presented. A six-port converter is presented that enables charge exchange both along each of the strings and between the strings in the hybrid energy storage. An analysis of converter operation demonstrates some promising features carrying out several necessary functions in multi cell, energy storage strings and provides some added value taking care of up to six cells, reducing significantly on the component number required. A single cycle conversion eliminates the double conversion required in similar cases. A theoretical foundation and an analysis are presented and validated using several approaches in PSIM simulation and experimentally. Four experimental trials were carried out, covering the operation of most of the hybrid energy storage system functionalities, and include the balancing of the batteries and the capacitors, linking between the string in both regular balancing and boost modes, and hybrid operation of the two strings in a presence of peak current demands. The experimental results are in an excellent agreement with the theoretical predictions.

References

[1] M. Quarti, A. Bayer, W.G. Bessler, “Trade-off between energy density and fast-charge capability of lithium-ion batteries: A model-based design study of cells with thick electrodes” , *Electrochem Sci Adv.*, Vol 3, 2023.

[2] Jürgen Wenig, Mariya Sodenkamp, Thorsten Staake, “Battery versus infrastructure: Tradeoffs between battery capacity and charging infrastructure for plug-in hybrid electric vehicles,” *Applied Energy*, Vol. 255, 2019.

[3] Park, S.-H., Tian, R., Coelho, J., Nicolosi, V., Coleman, J. N., “Quantifying the Trade-Off between Absolute Capacity and Rate Performance in Battery Electrodes,” *Adv. Energy Mater.* 2019.

[4] P. Thounthong, V. Chunkag, P. Sethakul, B. Davat and M. Hinaje, "Comparative Study of Fuel-Cell Vehicle Hybridization with Battery or Supercapacitor Storage Device," in *IEEE Transactions on Vehicular Technology*, vol. 58, no. 8, pp. 3892-3904, Oct. 2009.

[5] K. Abo-Elyousr, R. M. Kamel, H. Abo-zeid and F. Abd-elbar, "Characterization and effectiveness of an ultracapacitor bank to enhance a battery electric vehicle energy storage system dynamics," *2013 International Conference on Electrical Machines and Systems (ICEMS)*, Busan, Korea (South), 2013, pp. 235-241.

[6] X. Rui, H. Hongwen, Z. Xiaowei and W. Yi, "Simulation study on hybrid ultracapactior-battery power system for PHEV," *2010 2nd International Conference on Future Computer and Communication*, Wuhan, China, 2010, pp. V1-496-V1-500.

[7] Fanning Jin, Mengqi Wang and Changjian Hu, "A fuzzy logic based power management strategy for hybrid energy storage system in hybrid electric vehicles considering battery degradation," *2016 IEEE Transportation Electrification Conference and Expo (ITEC)*, Dearborn, MI, 2016, pp. 1-7.

[8] M. Evzelman, M. M. Ur Rehman, K. Hathaway, R. Zane, D. Costinett and D. Maksimovic, "Active Balancing System for Electric Vehicles With Incorporated Low-Voltage Bus," in *IEEE Transactions on Power Electronics*, vol. 31, no. 11, pp. 7887-7895, Nov. 2016.

[9] M. M. U. Rehman, F. Zhang, M. Evzelman, R. Zane, K. Smith and D. Maksimovic, "Advanced cell-level control for extending electric vehicle battery pack lifetime," *2016 IEEE Energy Conversion Congress and Expo. (ECCE)*, Milwaukee, WI, USA, 2016, pp. 1-8.

[10] I. Biswas, D. Kastha and P. Bajpai, "TAB Based Multiport Converter with Optimized Transformer RMS Current and Improved ZVS Range for DC Microgrid Applications," *IECON 2019 - 45th Annual Conference of the IEEE Industrial Electronics Society*, Lisbon, Portugal, 2019, pp. 2050-2055.

[11] M. Rasheed, H. Wang and R. Zane, "Analysis of a Five-Port Differential Power Processing Triple Active Bridge Converter for Active Cell Balancing in Lithium-ion Battery Packs," 2022 IEEE 23rd Workshop on Control and Modeling for Power Electronics (COMPEL), Tel Aviv, Israel, 2022, pp. 1-8.

[12] M. Rasheed et al., "Composite Hybrid Energy Storage System utilizing Capacitive Coupling for Hybrid and Electric Vehicles," 2021 IEEE Applied Power Electronics Conference and Exposition (APEC), AZ, USA, 2021, pp. 939-946..

[13] M. Rasheed, C. Simpson, H. Wang and R. Zane, "Multi-Loop Control of Hybrid Li-ion Battery Packs Using the Auxiliary DC Bus for State-of-Charge Regulation," 2022 IEEE Energy Conversion Congress and Exposition (ECCE), Detroit, MI, USA, 2022, pp. 1-8.

[14] F. Krismer, J. Biela, and J. W. Kolar, "A Comparative Evaluation of Isolated Bi-directional DC/DC Converters with Wide Input and Output Voltage Range," IEEE Industry Applications Conference, Fourteenth IAS Annual Meeting, vol. 1, pp. 599 - 606, 2-6 October 2005.

[15] I. Zeltser, “Analysis of a Low Power, High Voltage and High Gain Capacitor Charger with Output Sourcing Behavior,” IEEE Applied Power Electronics Conference and Exposition, APEC 2017, pp. 1640-1646.